

1 **Lineage and stage-specific expressed *CYCD7;1* coordinates the single symmetric division that**  
2 **creates stomatal guard cells**

3

4 Annika K. Weimer<sup>1,6</sup>, Juliana L. Matos<sup>1,2,6</sup>, Walter Dewitte<sup>3,4</sup>, James A.H. Murray<sup>3,4</sup>, Dominique C.  
5 Bergmann<sup>1,5,\*</sup>

6 <sup>1</sup> Department of Biology, Stanford University, Stanford, CA, USA

7 <sup>2</sup> Present address: University of California Berkeley, Plant and Microbial Biology, Berkeley, CA, USA

8 <sup>3</sup> Cardiff School of Bioscience, Cardiff University, Wales, United Kingdom

9 <sup>4</sup> Institute of Biotechnology, University of Cambridge, United Kingdom

10 <sup>5</sup> Howard Hughes Medical Institute (HHMI), Stanford University, Stanford, CA, USA

11 <sup>6</sup> These authors contributed equally to this work.

12 \* Author for correspondence: [dbergmann@stanford.edu](mailto:dbergmann@stanford.edu)

13

14 **Running title:** *CYCD7;1* triggers GMC divisions

15 **Keywords:** stomatal development, cell cycle, cyclin, cell division, differentiation, guard cell

16

17 **Summary statement:**

18 The core cell cycle component, *CYCD7;1* requires stomatal transcription factors for its GMC-specific  
19 expression; *CYCD7;1* promotes the single symmetric division that ensures production of a 2-celled  
20 stomatal complex.

21

22 **Abstract**

23 Plants, with cells fixed in place by rigid walls, often utilize spatial and temporally distinct cell division  
24 programs to organize and maintain organs. This leads to the question of how developmental regulators  
25 interact with the cell cycle machinery to link cell division events with particular developmental  
26 trajectories. In *Arabidopsis* leaves, the development of stomata, two-celled epidermal valves that  
27 mediate plant-atmosphere gas exchange, relies on a series of oriented stem-cell-like asymmetric  
28 divisions followed by a single symmetric division. The stomatal lineage is embedded in a tissue whose  
29 cells transition from proliferation to post-mitotic differentiation earlier, necessitating stomatal lineage-  
30 specific factors to prolong competence to divide. We show that the D-type cyclin, *CYCD7;1* is  
31 specifically expressed just prior to the symmetric guard-cell forming division, and that it is limiting for

32 this division. Further, we find that *CYCD7;1* is capable of promoting divisions in multiple contexts,  
33 likely through RBR-dependent promotion of the G1/S transition, but that *CYCD7;1* is regulated at the  
34 transcriptional level by cell-type specific transcription factors that confine its expression to the  
35 appropriate developmental window.

36

## 37 **Introduction**

38 Development of multicellular organisms requires the coordination and control of cell proliferation with  
39 differentiation programs to generate distinct cell types, tissues and organs. Different cell lineages are  
40 specified by sets of developmental regulators and display various cell proliferation dynamics, suggesting  
41 that the cell cycle machinery might not always be comprised of the same components or controlled in  
42 the same way. In *Arabidopsis*, the mature leaf epidermis contains pavement cells, trichomes and  
43 stomata, three different functional cell types with their own developmental trajectories. Trichome  
44 precursors are specified early and patterned via lateral inhibition networks (Schellmann et al., 2002), and  
45 their maturation requires a shift from mitotic to endoreplication programs (Bramsiepe et al., 2010).  
46 Pavement cells also endoreplicate as they acquire their lobed morphologies (Katagiri et al., 2016).

47

48 Stomata, pivotal for gas exchange between the plant and the environment, are derived from protodermal  
49 cells in a process that requires them to first become self-renewing and multi-potent, but then to navigate  
50 an ordered set of divisions and differentiation programs to create the mature stoma (Matos and  
51 Bergmann, 2014). Stomatal development requires three essential, stage-specific, basic-helix loop-helix  
52 (bHLH) transcription factors, *SPEECHLESS* (*SPCH*), *MUTE* and *FAMA* and their broadly expressed  
53 heterodimer partners *SCRM/ICE1* and *SCRM2* (Kanaoka et al., 2008) (Fig 1A). *SPCH* drives  
54 asymmetric cell divisions that initiate the lineage, creating meristemoids (M) that may undergo  
55 continued self-renewing divisions. Plants lacking *SPCH* have no stomatal lineage. *MUTE* is essential to  
56 terminate the asymmetric self-renewing divisions and to induce the differentiation of meristemoids into  
57 guard mother cells (GMCs) (MacAlister et al., 2007; Pillitteri et al., 2007); loss of *MUTE* results in  
58 excess meristemoids at the expense of GMCs (MacAlister et al., 2007; Pillitteri and Torii, 2007). *FAMA*  
59 is required for the establishment of GCs but also to restrict GMCs to a single division. *fama* mutants  
60 exhibit numerous rounds of symmetric and parallel GMC divisions without acquisition of terminal GC  
61 identities (Matos et al., 2014; Ohashi-Ito and Bergmann, 2006). Plants bearing mutations in two R2R3

62 MYB transcription factor genes *FOUR LIPS (FLP)* and *MYB88* also exhibit *fama*-like GMC over-  
63 proliferation phenotypes (Lai et al., 2005; Xie et al., 2010).

64

65 The varied trajectories of epidermal cells have been useful tools for dissecting cell cycle behaviors. The  
66 components of the core cell cycle machinery are highly conserved among eukaryotes, though there has  
67 been a large expansion of genes in plants (Harashima et al., 2013; Inzé and De Veylder, 2006). The plant  
68 cell cycle is regulated by 5 main cyclin-dependent kinases (CDKs), CDKA;1, CDKB1;1, CDKB1;2,  
69 CDKB2;1 and CDKB2;2. CDKs require cyclins (CYC) as binding partners for their kinase activity  
70 toward downstream phosphorylation targets. Plants genomes encode much larger families of cyclin  
71 genes than animals; for example, *Arabidopsis* encodes at least 32 cyclins (Vandepoele et al., 2002;  
72 Wang et al., 2004) and it has been speculated that this expansion allows plants to specifically regulate  
73 their postembryonic development (De Veylder et al., 2007; Harashima et al., 2013; Inzé and De Veylder,  
74 2006). D-type cyclins as partners of CDKA;1 are critical for the G1/S cell cycle transition and  
75 commitment to divide (Dewitte et al., 2007; Harbour and Dean, 2000; Riou-Khamlichi et al., 2000).  
76 Eight out of ten plant CYCDs have an RBR1-binding motif (LxCxE) (Kono et al., 2007; Menges et al.,  
77 2003). RBR1, the *Arabidopsis* homolog of the human tumor suppressor protein Retinoblastoma, is  
78 crucial for the negative control of the cell cycle at G1/S transition (Desvoyes et al., 2006; Gutzat et al.,  
79 2012; Nowack et al., 2012; Uemukai et al., 2005; Zhao et al., 2012). Phosphorylation of RBR1 by  
80 CDKA;1/CYCD complexes inactivates its suppression of E2F transcription factors, allowing entry into  
81 S phase and commitment to divide (Fig. 1B) (Harashima et al., 2013; Nakagami et al., 2002; Nowack et  
82 al., 2012; Umen and Goodenough, 2001).

83

84 Here we show how the cell cycle and cell fate transition from GMCs to GCs is regulated by the  
85 stomatal-lineage specific G1-S phase cell cycle regulator *CYCD7;1*. We demonstrate that *CYCD7;1*  
86 activity is that of a typical D-type cyclin, but its expression window is narrowed by stomatal lineage  
87 specific transcription factors. By examining how *CYCD7;1* works with the core cell-cycle machinery  
88 and with stomatal regulators, and by revealing the phenotypes upon loss and gain of *CYCD7;1* function,  
89 we link a core cell-cycle regulator with a specific differentiation process and show how a formative  
90 division is initiated but also restricted to allow “one and only one division” in GMCs to create a  
91 physiologically functional valve structure from its two identical daughters.

92

## 93 Results

### 94 **CYCD7;1 is expressed prior to the last symmetric division in the stomatal lineage**

95 Among the 10 known D-type cyclins in *Arabidopsis*, *CYCD7;1* was uniquely enriched in transcriptional  
96 profiles of Fluorescence Activated Cell Sorting (FACS) isolated cells of the late stomatal lineage  
97 (Adrian et al., 2015). We confirmed this predicted expression in GMCs with transcriptional and  
98 translational reporters (Fig. 1C-E) and observed that additional copies of *CYCD7;1-YFP* could force  
99 ectopic divisions in GCs, suggesting that the protein could play a role in regulating this division (Fig.  
100 1C, white arrowhead). A translational reporter, *pCYCD7;1:CYCD7;1-YFP*, was characterized previously  
101 as peaking in GMCs (Adrian et al., 2015); however, the identity of *CYCD7;1* expressing cells was only  
102 assessed by morphology. To refine the expression pattern, we co-expressed *pCYCD7;1:CYCD7;1-YFP*  
103 with CFP reporters for SPCH, MUTE and FAMA (Fig. 1F-N). SPCH-CFP and *CYCD7;1-YFP*  
104 expression appear to be mutually exclusive, suggesting that *CYCD7;1* is not expressed in meristemoids  
105 (Fig. 1F-H). MUTE-CFP and *CYCD7;1-YFP* overlap in some cells, but we also see cells expressing  
106 only MUTE or only *CYCD7;1*. Cells that only express MUTE had the morphology typical of  
107 meristemoids, suggesting that MUTE is expressed before *CYCD7;1* (Fig. 1I-K). When compared to  
108 FAMA expression, *CYCD7;1-YFP* appears to be expressed before FAMA-CFP in GMCs, briefly  
109 together with FAMA in newly divided GCs, and then disappears before FAMA in GCs (Fig. 1L-N).  
110 Thus, the expression of *CYCD7;1* in the stomatal lineage is temporally and spatially controlled and  
111 starts after MUTE expression and finishes before FAMA expression (Fig. 1A).

112

113 We did not observe expression of *CYCD7;1-YFP* in any vegetative tissue from the seedling stage  
114 through flowering (data not shown). In adult plants, *CYCD7;1-YFP* was expressed in pollen sperm cells  
115 at anthesis, but not in the vegetative nucleus (Fig. S1). The expression of a D-type cyclin (typically  
116 expressed at G1/S) is consistent with the observations that sperm cells undergo an extended S phase in  
117 mature pollen grains (Friedman, 1999; Zhao et al., 2012).

118

119 Why does *CYCD7;1* have such a restricted expression pattern in the stomatal lineage? One possible  
120 explanation is that *CYCD7;1* has a unique function in GMC divisions. A second possibility is that  
121 *CYCD7;1* has a canonical role, i.e. it acts like other cyclins in promoting cell divisions, but it is  
122 important to be able to tightly control deployment of that role in the stomatal lineage. To distinguish  
123 between these models, we characterized plants missing or misexpressing *CYCD7;1*, tested relationships

124 between *CYCD7;1* and other cell cycle regulators, and defined how *CYCD7;1* expression was  
125 constrained by stomatal lineage transcription factors.

126

### 127 **Ectopic expression of *CYCD7;1* triggers divisions while *cycd7;1* mutants decelerate GMC** 128 **divisions**

129 If *CYCD7;1* has canonical CYCD activity, it should be able to promote cell divisions outside its normal  
130 expression window. To test this, we expressed *CYCD7;1* and *CYCD7;1*-YFP with the pan-epidermal  
131 promoter, ML1 (Roeder et al., 2010). Ectopic expression of *CYCD7;1* (YFP-tagged or untagged)  
132 induced cell divisions of pavement cells in the leaf (Fig. 2A-C) indicating that *CYCD7;1* can function as  
133 a canonical D-type cyclin.

134

135 Next, we asked if mutations of *CYCD7;1* result in abnormal phenotypes. We obtained multiple alleles of  
136 *CYCD7;1*: FLAG\_369E02 (*cycd7;1-1* (Collins et al., 2012), FLAG\_498H08 (*cycd7;1-2*), GK\_496G06-  
137 019628, SALK\_068526 and SALK\_068526 (Fig. S2A). We determined by qRT-PCR that *cycd7;1-1*  
138 (FLAG\_369E02) produced no transcript (Fig. S2B). On a whole plant level, we could not detect any  
139 abnormalities in *cycd7;1-1* compared to wild type (Fig. S1C). Because CYCDs promote G1/S transitions  
140 and *CYCD7;1* is specifically expressed during the GMC divisions, we asked whether *cycd7;1-1* mutants  
141 halt this transition by counting GCs in cotyledons. Mutants in *cycd7;1-1* do not display fewer GCs  
142 compared to wild type 7 days after germination (dag) (Fig. S2D-F). However, at 4 dag, when cells in the  
143 earlier stages of the stomatal lineage are abundant, *cycd7;1-1* cotyledons have more GMCs compared to  
144 wild type cotyledons (Fig. 2D). Interestingly, the average size of *cycd7;1-1* GMCs is larger than wild  
145 type (Fig. 2E). We confirmed that these GMC abundance and size phenotypes were present in plants  
146 bearing a different allele of *CYCD7;1* (*cycd7;1-2*) (Fig. S2G, H). Plant cells are known to increase in  
147 size during G1, so this phenotype suggests that *CYCD7;1* hastens cell cycle progression in the GMC to  
148 GC transition. Because *cycd7;1-1* is the null allele, we characterized its phenotypes in more detail. We  
149 introgressed *pCDKB1;1:GUS*, which labels the transition from GMC to GCs (Boudolf et al., 2004), into  
150 *cycd7;1-1* mutants. Compared to wild type, *cycd7;1-1* mutants show increased number of GUS-positive  
151 cells suggesting that these cells remain longer in GMC fate before they divide into GCs (Fig. 2F-H). To  
152 directly test this hypothesis, we labeled S phases with 5-ethynyl-2'-deoxyuridine (EdU) a thymidine  
153 analogue readily incorporated during DNA replication (Fig. 2I, J). Strikingly, significantly fewer GMCs  
154 in *cycd7;1-1* showed EdU labeling (indicating that they were in S phase during the EdU pulse)

155 compared to wild-type GMCs (Fig. 2K). Together these data suggest that CYCD7;1 is required for  
156 GMCs to make a timely entry into S phase before their transition into GCs.

157

### 158 **CYCD7;1 interacts with RBR1**

159 Typically, CYCDs drive the G1/S transition through inactivation of RBR1, and RBR1 activity was  
160 previously shown to be essential for repressing divisions in the stomatal lineage (Borghini et al., 2010;  
161 Matos et al., 2014). If CYCD7;1 and RBR1 function together, we would expect them to be co-  
162 expressed, to physically interact, and for there to be a phenotypic consequence of disrupting the  
163 interaction. Indeed, CYCD7;1 and RBR1 were shown to physically interact in BIFC and Y2H assays,  
164 dependent on the presence of the RBR1 binding motif LxCxE in CYCD7;1 (Matos et al., 2014). In  
165 addition, CYCD7;1 and RBR1 are co-expressed in GMCs (Fig. 3A-C). To test whether this interaction is  
166 functionally important, we took advantage of the fact that our translational reporter of CYCD7;1 triggers  
167 extra cell divisions in GCs (Fig. 1C, Fig. 3 D,E). Approximately 24% of GCs have one and 18% have  
168 two ectopic divisions in *pCYCD7;1:CYCD7;1-YFP* plants at 5 dag (Fig. 3G). If the RBR1 interaction is  
169 important for CYCD7;1 function, then mutation of the RBR1 binding motif LxCxE into LxGxK in  
170 CYCD7;1, should abrogate this division promoting activity. Strikingly, we found that  
171 *pCYCD7;1:CYCD7;1<sup>LGK</sup>-YFP* no longer triggers ectopic cell divisions in GCs (Fig. 3F,G). This effect  
172 was not due to differences in expression levels between *CYCD7;1-YFP* and *CYCD7;1<sup>LGK</sup>-YFP* (Fig  
173 S1B). Production of ectopic cell divisions in GCs, therefore, depends on the RBR1 binding residues in  
174 CYCD7;1.

175

### 176 **CYCD7;1 needs CDKB1 activity to drive ectopic divisions**

177 Cyclins bind to CDKs to ensure kinase activity and completion of cell division; undivided cells  
178 expressing GC fate markers result from reduction or loss of CDK activity (e.g., hypomorphic *cdka;1*  
179 mutants (Weimer et al., 2012), *cdkb1;1 cdkb1;2* double mutants (Xie et al., 2010) or dominant-negative  
180 CDKB1;1-N161 (Boudolf et al., 2004)). To test whether CYCD7;1 required CDK activity to drive  
181 divisions, we expressed CYCD7;1-YFP and CYCD7;1<sup>LGK</sup>-YFP under the CYCD7;1 promoter in plants  
182 bearing a dominant negative version of *CDKB1;1* (CDKB1;1-N161, Fig. 3H-J). Although we could see  
183 expression of both CYCD7;1 markers in arrested GMCs, they could neither rescue the phenotype nor  
184 trigger ectopic cell divisions (Fig. 3I-K). Thus CYCD7;1 requires CDKB1 activity either as a partner, or  
185 downstream at the G2/M transition for completion of the division.

186 **CYCD7;1 expression domain is constrained by stomatal lineage transcription factors**

187 Our evidence points to CYCD7;1 acting like a canonical CYCD, therefore we turned our attention to  
188 regulation of its highly restricted expression pattern. Three transcription factors are contemporaneously  
189 expressed with CYCD7;1—MUTE, FAMA and FLP (Fig 1I-K)—but MUTE precedes CYCD7;1 while  
190 the others persist longer. Given these patterns, we tested whether MUTE was necessary for CYCD7;1  
191 expression. When *pCYCD7;1:CYCD7;1-YFP* was crossed into the *mute* mutant, we could observe the  
192 typical *mute* phenotype of many small meristemoid-like cells that fail to differentiate into GMCs  
193 (Pillitteri et al., 2007). In a few of these meristemoid-like cells, we detected weak CYCD7;1-YFP signal  
194 (Fig. 4A,B). Fluorescence intensity measurements showed that CYCD7;1-YFP signals in *mute* are ~50%  
195 reduced (Fig 4C-F) indicating that MUTE promotes CYCD7;1 expression, though it is not absolutely  
196 essential for it. In none of these images did we observe any ectopic divisions of the meristemoid-like  
197 cells.

198

199 CYCD7;1 appears to be repressed during FAMA's expression peak. We therefore tested whether  
200 FAMA, in its role as the master transcriptional regulator of stomatal division and differentiation, is a  
201 direct regulator of CYCD7;1. In *fama* mutants GMCs divide repeatedly without attaining GC fate (Fig.  
202 5A-E) and these “tumors” express CYCD7;1-YFP (Fig. 5B,C); although the reporter fades in older  
203 leaves suggesting that CYCD7;1-YFP is also subject to posttranslational regulation (Fig. 5D,E). In the  
204 *fama* tumors, *pCYCD7;1:CYCD7;1-YFP* drives ectopic divisions (Fig. 5B,D, white arrowheads), but the  
205 *CYCD7;1<sup>LGK</sup>* version that cannot bind RBR1, does not (Fig. 5C,E). To test whether FAMA might  
206 directly regulate CYCD7;1, we extracted reads from a FAMA ChIP-seq experiment, performed under  
207 similar conditions as in (Lau and Bergmann, 2015; Lau et al., 2014). As shown in Fig. 5F, it is clear that  
208 FAMA is associated with the promoter region and gene body of *CYCD7;1*.

209

210 Along with FAMA, two partially redundant R2R3 MYB transcription factors, FOUR LIPS (FLP) and  
211 MYB88, restrict GMC divisions. Previously, it was shown that FLP/MYB88 bind directly to the  
212 *CDKBI;1* promoter and can repress *CDKBI;1* transcription (Lee et al., 2013; Vanneste et al., 2011; Xie  
213 et al., 2010). *flp/myb88* mutants also display GMC overproliferation but, unlike *fama* mutants, some  
214 differentiated GCs form (Lai et al., 2005; Xie et al., 2010), Fig. 4F,I). *CYCD7;1-YFP* (and *CYCD7;1<sup>LGK</sup>-*  
215 *YFP*) translational reporters are highly expressed in *flp/myb88*, and CYCD7;1-YFP, but not  
216 *CYCD7;1<sup>LGK</sup>-YFP*, induces ectopic divisions (Fig. 4 G,H,J,K).

217 The phenotypes of loss and gain of *CYCD7;1* activity suggest that its narrow window of expression is  
218 essential to guarantee a 2-celled stomatal complex. Using the *FAMA* promoter in wild type, thus driving  
219 *CYCD7;1* slightly later than under its endogenous cis-regulatory control, we find a dramatic  
220 enhancement of ectopic divisions (Fig. 5G-K). Compared to *pCYCD7;1:CYCD7;1-YFP* in which ~24%  
221 of stomata were four-celled at 5 dag, in *pFAMA:CYCD7;1-YFP*, that number was ~70%, with 2% of  
222 stomata being 8-celled (N=237). The amount of four-celled stomata increases to 87% at 12 dag, with  
223 another 2% being 8-celled (N=153). (Fig. 5K). Quantification of fluorescence intensity indicates that  
224 expression with *FAMA* and *CYCD7* promoters yields equivalent levels of *CYCD7;1-YFP* in GMCs (Fig  
225 S1B), however, this fusion protein persists in ectopically divided GCs when expressed under the *FAMA*  
226 promoter (Fig. 5L). This directly links the activity of *FAMA* as a lineage specific transcription factor  
227 with the cell cycle regulator *CYCD7;1* to ensure “one and only one division” to create a pair of guard  
228 cells.

229

## 230 Discussion

231 We have shown that *CYCD7;1* is specifically expressed in GMCs prior to the last symmetric cell  
232 division that forms the 2-celled stomatal complex. Depletion of *CYCD7;1* slows down this cell division  
233 whereas ectopic expression of *CYCD7;1* can trigger cell divisions in GCs. Mutation of the RBR1  
234 binding motif in *CYCD7;1* disrupts its interaction with RBR1 and renders *CYCD7;1<sup>LGK</sup>* incapable of  
235 driving ectopic division. The connection to RBR1 fits with previous work showing that *CYCD7;1*  
236 interacts with *CDKA;1* (Van Leene et al., 2010), together supporting a role for *CYCD7;1* in the  
237 canonical regulatory complex for G1/S transitions and the commitment to divide. *CYCD7;1* activity in  
238 cell cycles, however, is directly repressed by the lineage specific transcription factor *FAMA* to ensure a  
239 coupling between the cell division which terminates the stomatal lineage, and the formation of  
240 terminally fated GCs. This interconnection represents a direct link between cell cycle regulators and  
241 developmental decisions (Fig. 6).

242

243 *CYCDs* are critical for the G1/S transition and commitment to divide, and are therefore interesting  
244 candidate hubs for the integration of developmental control with the cell cycle machinery. In  
245 *Arabidopsis*, there are 10 D-type cyclins, some active in multiple tissues (*CYCD3s*, *CYCD4s*,  
246 *CYCD2;1*) but others whose activity is linked to specific cell types (*CYCD6;1* and *CYCD7;1*) or cell  
247 cycle behaviors (*CYCD5;1* endoreplication) (Dewitte et al., 2007; Kono et al., 2007; Sanz et al., 2011;



248 Sterken et al., 2012) (Adrian et al., 2015; Sozzani et al., 2010), this study). Phylogenetic analyses  
249 showed that *CYCD6;1* and *CYCD7;1* proteins diverge from other D-type cyclins in *Arabidopsis* (Wang  
250 et al., 2004), but also that *CYCD7;1* most closely resembles the single D-type cyclin in *Physcomitrella*  
251 (Menges et al., 2007), consistent with our observation that it could promoting G1/S transitions (a core  
252 D-type activity) in multiple cell types.

253

254 Interestingly, both *CYCD6;1* and *CYCD7;1* are limiting for essential formative divisions during  
255 development. In the root, *CYCD6;1* is important for the cortex endodermis initial daughter (CEID) cell  
256 divisions (Sozzani et al., 2010; Weimer et al., 2012). Here, *SHORTROOT* (*SHR*) directly activates  
257 expression of *CYCD6;1* which works in concert with *CDKA;1* to trigger the formative division of the  
258 CEID (Cruz-Ramírez et al., 2012; Sozzani et al., 2010; Weimer et al., 2012). This interaction promotes  
259 the initiation of an asymmetric stem-cell division program. In contrast, *CYCD7;1* expression marks the  
260 boundary between two types of divisions: the continual asymmetric divisions of meristemoids vs. the  
261 single symmetric division of a GMC. Here we find a quantitative requirement for *MUTE* to promote full  
262 *CYCD7;1* expression, but a clear requirement for *FAMA* and *FLP/MYB88* to repress *CYCD7;1* after  
263 GMC division. The low expression level of *CYCD7;1* in the absence of *MUTE* may point to a direct role  
264 for *MUTE* in activating *CYCD7;1* expression. *MUTE* is structurally similar to *FAMA*, and therefore  
265 might be able to interact with *CYCD7;1* regulatory sequences. Alternatively, as meristemoid cells in  
266 *mute* never transition into GMCs, low *CYCD7;1* levels may be an indirect consequence of altered cell  
267 fate. In either case, it is notable that the introduction of *CYCD7;1*-YFP in *mute* did drive not additional  
268 meristemoid cell divisions suggesting that *CYCD7;1*'s division-promoting behavior requires a threshold  
269 level not reached in this genetic background.

270

271 It is tempting to speculate that spatiotemporal restriction of *CYCDs* could be a mechanism to control the  
272 cell cycle machinery more efficiently and to cope with different developmental programs. The  
273 importance of these specialized *CYCDs*, however, must be squared with the relatively minor phenotypes  
274 associated with their loss—neither *CYCD7;1* nor *CYCD6;1* mutants abolish the production of  
275 specialized cells or tissue layers (Fig. 2) (Sozzani et al., 2010)). Most likely, *CYCD6;1* and *CYCD7;1*  
276 assist other, more general, cyclins in executing the cell division programs or ensure particularly high cell  
277 cycle kinase activity. In the case of the stomatal lineage, *CYCD3;1* and *CYCD3;2*, despite being  
278 considered general G1/S cyclins (Dewitte et al., 2007; Dewitte et al., 2003; Menges et al., 2006), also

279 show high expression in the stomatal lineage (Adrian et al., 2015). It is also important to recognize that  
280 CYCD/CDKA complexes likely have many downstream targets and that increased kinase activity could  
281 induce different downstream processes, either in a feedback loop or for differentiation processes. In  
282 plants, specific CDK/cyclin complexes can have differential activity towards individual substrates, and  
283 both CDK and cyclin proteins contribute to substrate recognition (Harashima and Schnittger, 2012),  
284 however, there is evidence that between the CDK and cyclin, the cyclin may have a more prominent role  
285 (Weimer et al., 2016). Specific expression of individual cyclins, such as CYCD7;1 in the stomatal  
286 lineage, therefore, could contribute to fine-tuning of cell division control and downstream substrate  
287 recognition.

288

289 Leaves lose overall division competency as they mature, leading to a situation where GMCs are  
290 surrounded by post-mitotic cells. Formation of functional stomata, however, requires a cell division to  
291 produce two cells, suggesting that this division has unique additional regulation. Stomata are found in  
292 remarkably diverse patterns and exhibit a 10-fold variation in size in different species (McElwain et al.,  
293 2016), yet there have still to be reports of more than two stomatal guard cells flanking a pore. Therefore,  
294 despite the ease with which we could create four-celled stomata through experimental manipulation, in  
295 nature, regulation to ensure a single division appears crucial.

## 296 **Material and Methods**

### 297 **Plant material and growth conditions**

298 *Arabidopsis thaliana* Columbia-0 (Col-0) was used as wild type in all experiments. All mutants and  
299 transgenic lines tested have this ecotype background. Seedlings were grown on half-strength Murashige  
300 and Skoog (MS) medium (Caisson labs, USA) medium at 22°C under 16 hour-light/8 hour-dark cycles  
301 and were examined at the indicated time. The following previously described mutants and reporter lines  
302 were used in this study: *mute* (Pillitteri et al., 2007); *fama-1* (Ohashi-Ito and Bergmann, 2006);  
303 *flp;myb88* (Lai et al., 2005); *proSPCH:SPCH:CFP* and *proMUTE:MUTE-YFP* (Davies and Bergmann,  
304 2014); *proRBRI:RBRI-CFP* (Cruz-Ramírez et al., 2012), *pro35S:CDKB1;1-N161* (Boudolf et al.,  
305 2004); *proCDKB1;1:GUS* (Boudolf et al., 2004).

306

### 307 **CYCD7;1 mutants**

308 CYCD7;1 mutants FLAG\_369E02 (*cycd7;1-1*) and FLAG\_498H08 (*cycd7;1-2*) were derived from the  
309 INRA/Versaille collection (Versaille, France) and *cycd7;1;1* was backcrossed twice to Col-0.  
310 GK\_496G06-019628 was derived from the GABI-Kat collection (Cologne, Germany). SALK\_068423  
311 and SALK\_068526 were obtained from ABRC (Columbus, USA).

312

### 313 **Vector construction and plant transformation**

314 Constructs were generated using the Gateway® system (Invitrogen, CA, USA). Appropriate genome  
315 sequences (PCR amplified from Col-0 or from entry clones) were cloned into Gateway compatible entry  
316 vectors, typically pENTR/D-TOPO (Life Technologies, CA, USA), to facilitate subsequent cloning into  
317 plant binary vectors pHGY (Kubo et al., 2005) or R4pGWB destination vector system (Nakagawa et al.,  
318 2008; Tanaka et al., 2011). The translational reporter for CYCD7;1 was generated by cloning the  
319 genomic fragment (promoter+CDS) into the entry vector pENTR to generate the entry vector CYCD7;1-  
320 genomic-pENTR, followed by LR recombination into the destination vector pHGY to generate the final  
321 construct. For the translational reporter for CYCD7;1<sup>LGK</sup>, the LxCxE motif of CYCD7;1-genomic-  
322 pENTR was mutated to LxGxK by site directed mutagenesis using the QuikChange II Kit (Agilent, CA,  
323 USA) to generate the entry clone CYCD7;1-genomic-pENTR and then recombined into pHGY. The  
324 transcriptional reporters for CYCD7;1 were generated by cloning the CYCD7;1 promoter region into  
325 pENTR, then recombined into the destination vectors pHGY (cytosolic YFP). The other constructs  
326 generated in this study *proCYCD7;1:YFP-YFPnls*, *proFAMA:FAMA-CFP*, *proML1:CYCD7;1-YFP*,

327 *proML1:CYCD7;1*, *proCYCD7;1:CYCD7;1*, and *proFAMA:CYCD7;1-YFP* were generated with the  
328 tripartite recombination of the plant binary vector series R4pGWB (Nakagawa et al., 2008; Tanaka et  
329 al., 2011), with the Gateway entry clones of the promoters and coding sequences compatible with the  
330 binary R4pGWB destination vector system. Primer sequences used for entry clones are provided in  
331 Table 1. Transgenic plants were generated by Agrobacterium-mediated transformation (Clough, 2005)  
332 and transgenic seedlings were selected by growth on half-strength MS plates supplemented with 50  
333 mg/L Hygromycin (pHGY, p35HGY, pGWB1, pGWB540 based constructs) or Kanamycin 100 mg/L  
334 (pGWB440 and pGWV401 based constructs) or 12 mg/L of Basta (pGWB640 based constructs).

335

### 336 **Confocal and DIC microscopy**

337 For confocal microscopy, images were taken with a Leica SP5 microscope and processed in ImageJ.  
338 Cell outlines were visualized by either 0.1 mg/ml propidium iodide in water (Molecular Probes, OR,  
339 USA) incubation for 10 min, rinsed in H<sub>2</sub>O once). For DIC microscopy, samples were cleared in 7:1  
340 ethanol:acetic acid, treated 30 min with 1N potassium hydroxide, rinsed in water, and mounted in  
341 Hoyer's medium. Differential contrast interference (DIC) images were obtained from the middle region  
342 of adaxial epidermis of cotyledons on a Leica DM2500 microscope or Leica DM6 B microscope.

343

### 344 **Quantification of fluorescent intensity**

345 Images of GMCs in cotyledons were taken at 4 dag with identical settings and processed in ImageJ.  
346 Fluorescent intensity was measured as mean gray value in the nucleus, subtracted by the background.  
347 Measurements were averaged for mutant and control experiments with Student's-t-test used to determine  
348 the statistical significance.

349

### 350 **GUS staining**

351 5-day old seedlings were incubated in staining solution for 12 hours and destained in 70% ethanol at 60–  
352 70°C for four hours. Staining solution for 5ml: 100µl of 10% Triton X-100, 250µl 1M NaPO<sub>4</sub> (pH 7.2),  
353 100µl 100mM potassium ferrocyanide, 100µl potassium ferricyanide, 400µl 25 mM X-Gluc, 4050µl  
354 dH<sub>2</sub>O. Images were taken with a Leica DM6 B microscope.

355

356

357

## 358 **EdU labeling**

359 EdU labeling was performed using the Click-iT® EdU Alexa Fluor® 488 Imaging Kit (ThermoFisher  
 360 Scientific, MA, USA). 4-day old seedlings were incubated in 20µM EdU solution in half-strength MS  
 361 for 90 minutes at room temperature. Seedlings were transferred to new tubes and washed three times  
 362 with wash buffer (1% BSA in PBS). Wash buffer was removed and fixation buffer was added (3.7%  
 363 formaldehyde in PBS) for 30 min at room temperature. Seedlings were transferred to new tubes and  
 364 washed two times with permeabilization buffer (0.5% Triton x-100 in PBS) for 10 minutes each,  
 365 protected from light on a slow rocking platform. Plants were transferred to new tubes and incubated in  
 366 reaction cocktail (455µL Click-IT reaction buffer, 20µL CuSO<sub>4</sub>, 2µL Alexa Fluor Azide 488, 25 µL 1x  
 367 Click-IT EdU additive) for 1 hour at room temperature, protected from light, without agitation.  
 368 Seedlings were transferred to new tubes and washed twice for 10 minutes at room temperature with  
 369 wash buffer on a slow rocking platforms, protected from light. Cotyledons were imaged using a Leica  
 370 SP5 microscope not more than two hours after the completion of washes and processed in ImageJ.

371

## 372 **qPCR**

373 100 mg ground frozen material from 8-day old plants was used for RNA extraction according to the  
 374 manufacture's manual (RNeasy Mini Kit, Qiagen, Germany). 1µg total RNA was used as a template for  
 375 cDNA synthesis (iScript cDNA synthesis kit, BioRad, CA, USA). qPCR setup was according to the  
 376 manual of the SsoAdvanced Universal SYBR Green Supermix (BioRad, CA, USA). qPCR was  
 377 performed by CFX96 Real Time C1000 Thermal Cycler (BioRad, CA, USA) according to the following  
 378 reaction conditions: 95°C for 30 s, followed by 39 cycles at 95°C for 10 s and at 60°C for 30 s. ACTIN  
 379 was used as a reference gene for all qPCRs performed. Primers can be found in Table 1.

380

381 **Table 1: Primers used in this study.**

	Forward primer (5'-3')	Reverse primer
CYCD7 genomic region (promoter + CDS)	CACCGAGAACTATAGTAGAAGGAAAC	AATGTAATTTGACATTTCAATTG
CYCD7;1 <sup>LGK</sup> genomic	TAATCTACTCGGAGAAAAATCTTGGCCCGAGTCC	CTCGGGGCAAGATTTTTCTCCGAGTAG ATTATCC
CYCD7;1 promoter	CACCGAGAACTATAGTAGAAGGAAAC	GCGCCGCTTGAAACTGAACCGGTTT
CYCD7;1 genomic	CACCATGGATAATCTACTCTGCGAAG	AATGTAATTTGACATTTCAATTG
CYCD7;1 <sup>LGK</sup> genomic	CACCATGGATAATCTACTCTGCGAAG	AATGTAATTTGACATTTCAATTG
CYCD7;1 qPCR	TCCATGCGTTTCAATGGCTAATCC	TCCACCATCCAATTCGTCCATTCC
ACTIN qPCR	CAAGGCCGAGTATG	GAAACGCAGACGTA
<i>cycd7;1-1</i> RB T-DNA	CCAGACTGAATGCCACAGGCCGTC	

CYCD7;1	ATGGATAATCTACTCTGCGA	AATGTAATTTGACATTTCAATTG
---------	----------------------	-------------------------

382

383

384 **Acknowledgments**

385 We thank members of the Bergmann lab for helpful comments on the manuscript and Charles Hachez  
386 (UCLouvain) for his contributions to the initiation of the CYCD7;1 project.

387

388

389 **Competing Interests**

390 The authors declare no competing or financial interest.

391 **Funding**

392 AKW is supported by a postdoctoral fellowship from the German Research Foundation (DFG). DCB is  
393 an investigator of the Howard Hughes Medical Institute.

394 **References**

- 395 **Adrian, J., Chang, J., Ballenger, C. E., Bargmann, B. O. R., Alassimone, J., Davies, K. A., Lau, O.**  
396 **S., Matos, J. L., Hachez, C., Lanctot, A., et al.** (2015). Transcriptome dynamics of the stomatal  
397 lineage: birth, amplification, and termination of a self-renewing population. *Dev. Cell* **33**, 107–118.
- 398 **Borghi, L., Gutzat, R., Fütterer, J., Laizet, Y., Hennig, L. and Gruissem, W.** (2010). Arabidopsis  
399 RETINOBLASTOMA-RELATED is required for stem cell maintenance, cell differentiation, and  
400 lateral organ production. *Plant Cell* **22**, 1792–1811.
- 401 **Boudolf, V., Barrôco, R., Engler, J. de A., Verkest, A., Beeckman, T., Naudts, M., Inzé, D. and De**  
402 **Veylder, L.** (2004). B1-type cyclin-dependent kinases are essential for the formation of stomatal  
403 complexes in Arabidopsis thaliana. *Plant Cell* **16**, 945–955.
- 404 **Bramsiepe, J., Wester, K., Weinl, C., Roodbarkelari, F., Kasili, R., Larkin, J. C., Hülskamp, M.**  
405 **and Schnittger, A.** (2010). Endoreplication controls cell fate maintenance. *PLoS Genet.* **6**,  
406 e1000996.
- 407 **Clough, S. J.** (2005). Floral dip: agrobacterium-mediated germ line transformation. *Methods Mol. Biol.*  
408 **286**, 91–102.
- 409 **Collins, C., Dewitte, W. and Murray, J. A. H.** (2012). D-type cyclins control cell division and  
410 developmental rate during Arabidopsis seed development. *J. Exp. Bot.* **63**, 3571–3586.
- 411 **Cruz-Ramírez, A., Díaz-Triviño, S., Blilou, I., Grieneisen, V. A., Sozzani, R., Zamioudis, C.,**  
412 **Miskolczi, P., Nieuwland, J., Benjamins, R., Dhonukshe, P., et al.** (2012). A bistable circuit  
413 involving SCARECROW-RETINOBLASTOMA integrates cues to inform asymmetric stem cell  
414 division. *Cell* **150**, 1002–1015.
- 415 **Davies, K. A. and Bergmann, D. C.** (2014). Functional specialization of stomatal bHLHs through  
416 modification of DNA-binding and phosphoregulation potential. *PNAS* **111**, 15585–15590.
- 417 **De Veylder, L., Beeckman, T. and Inzé, D.** (2007). The ins and outs of the plant cell cycle. *Nat. Rev.*  
418 *Mol. Cell Biol.* **8**, 655–665.
- 419 **Desvoyes, B., Ramirez-Parra, E., Xie, Q., Chua, N.-H. and Gutierrez, C.** (2006). Cell Type-Specific  
420 Role of the Retinoblastoma/E2F Pathway during Arabidopsis Leaf Development. *Plant Physiol.*  
421 **140**, 67–80.
- 422 **Dewitte, W., Riou-Khamlichi, C., Scofield, S., Healy, J. M. S., Jacquard, A., Kilby, N. J. and**  
423 **Murray, J. A. H.** (2003). Altered cell cycle distribution, hyperplasia, and inhibited differentiation in  
424 Arabidopsis caused by the D-type cyclin CYCD3. *The Plant Cell* **15**, 79–92.
- 425 **Dewitte, W., Scofield, S., Alcasabas, A. A., Maughan, S. C., Menges, M., Braun, N., Collins, C.,**  
426 **Nieuwland, J., Prinsen, E., Sundaresan, V., et al.** (2007). Arabidopsis CYCD3 D-type cyclins  
427 link cell proliferation and endocycles and are rate-limiting for cytokinin responses. *PNAS* **104**,  
428 14537–14542.
- 429 **Friedman, W. E.** (1999). Expression of the cell cycle in sperm of Arabidopsis: implications for

- 430 understanding patterns of gametogenesis and fertilization in plants and other eukaryotes.  
431 *Development* **126**, 1065–1075.
- 432 **Gutzat, R., Borghi, L. and Gruissem, W.** (2012). Emerging roles of RETINOBLASTOMA-  
433 RELATED proteins in evolution and plant development. *Trends Plant Sci.* **17**, 139–148.
- 434 **Harashima, H. and Schnittger, A.** (2012). Robust reconstitution of active cell-cycle control complexes  
435 from co-expressed proteins in bacteria. *Plant Methods* **8**, 23.
- 436 **Harashima, H., Dissmeyer, N. and Schnittger, A.** (2013). Cell cycle control across the eukaryotic  
437 kingdom. *Trends in Cell Biology* **23**, 345–356.
- 438 **Harbour, J. W. and Dean, D. C.** (2000). The Rb/E2F pathway: expanding roles and emerging  
439 paradigms. *Genes Dev.* **14**, 2393–2409.
- 440 **Inzé, D. and De Veylder, L.** (2006). Cell cycle regulation in plant development. *Annu. Rev. Genet.* **40**,  
441 77–105.
- 442 **Kanaoka, M. M., Pillitteri, L. J., Fujii, H., Yoshida, Y., Bogenschutz, N. L., Takabayashi, J., Zhu,  
443 J.-K. and Torii, K. U.** (2008). SCREAM/ICE1 and SCREAM2 specify three cell-state transitional  
444 steps leading to arabidopsis stomatal differentiation. *Plant Cell* **20**, 1775–1785.
- 445 **Katagiri, Y., Hasegawa, J., Fujikura, U., Hoshino, R., Matsunaga, S. and Tsukaya, H.** (2016). The  
446 coordination of ploidy and cell size differs between cell layers in leaves. *Development* **143**, 1120–  
447 1125.
- 448 **Kono, A., Umeda-Hara, C., Adachi, S., Nagata, N., Konomi, M., Nakagawa, T., Uchimiya, H. and  
449 Umeda, M.** (2007). The Arabidopsis D-type cyclin CYCD4 controls cell division in the stomatal  
450 lineage of the hypocotyl epidermis. *Plant Cell* **19**, 1265–1277.
- 451 **Kubo, M., Udagawa, M., Nishikubo, N., Horiguchi, G., Yamaguchi, M., Ito, J., Mimura, T.,  
452 Fukuda, H. and Demura, T.** (2005). Transcription switches for protoxylem and metaxylem vessel  
453 formation. *Genes Dev.* **19**, 1855–1860.
- 454 **Lai, L. B., Nadeau, J. A., Lucas, J., Lee, E.-K., Nakagawa, T., Zhao, L., Geisler, M. and Sack, F. D.**  
455 (2005). The Arabidopsis R2R3 MYB proteins FOUR LIPS and MYB88 restrict divisions late in the  
456 stomatal cell lineage. *Plant Cell* **17**, 2754–2767.
- 457 **Lau, O. S. and Bergmann, D. C.** (2015). MOBE-ChIP: a large-scale chromatin immunoprecipitation  
458 assay for cell type-specific studies. *Plant J.* **84**, 443–450.
- 459 **Lau, O. S., Davies, K. A., Chang, J., Adrian, J., Rowe, M. H., Ballenger, C. E. and Bergmann, D.  
460 C.** (2014). Direct roles of SPEECHLESS in the specification of stomatal self-renewing cells.  
461 *Science* **345**, 1605–1609.
- 462 **Lee, E., Liu, X., Eglit, Y. and Sack, F.** (2013). FOUR LIPS and MYB88 conditionally restrict the G1/S  
463 transition during stomatal formation. *J. Exp. Bot.* **64**, 5207–5219.

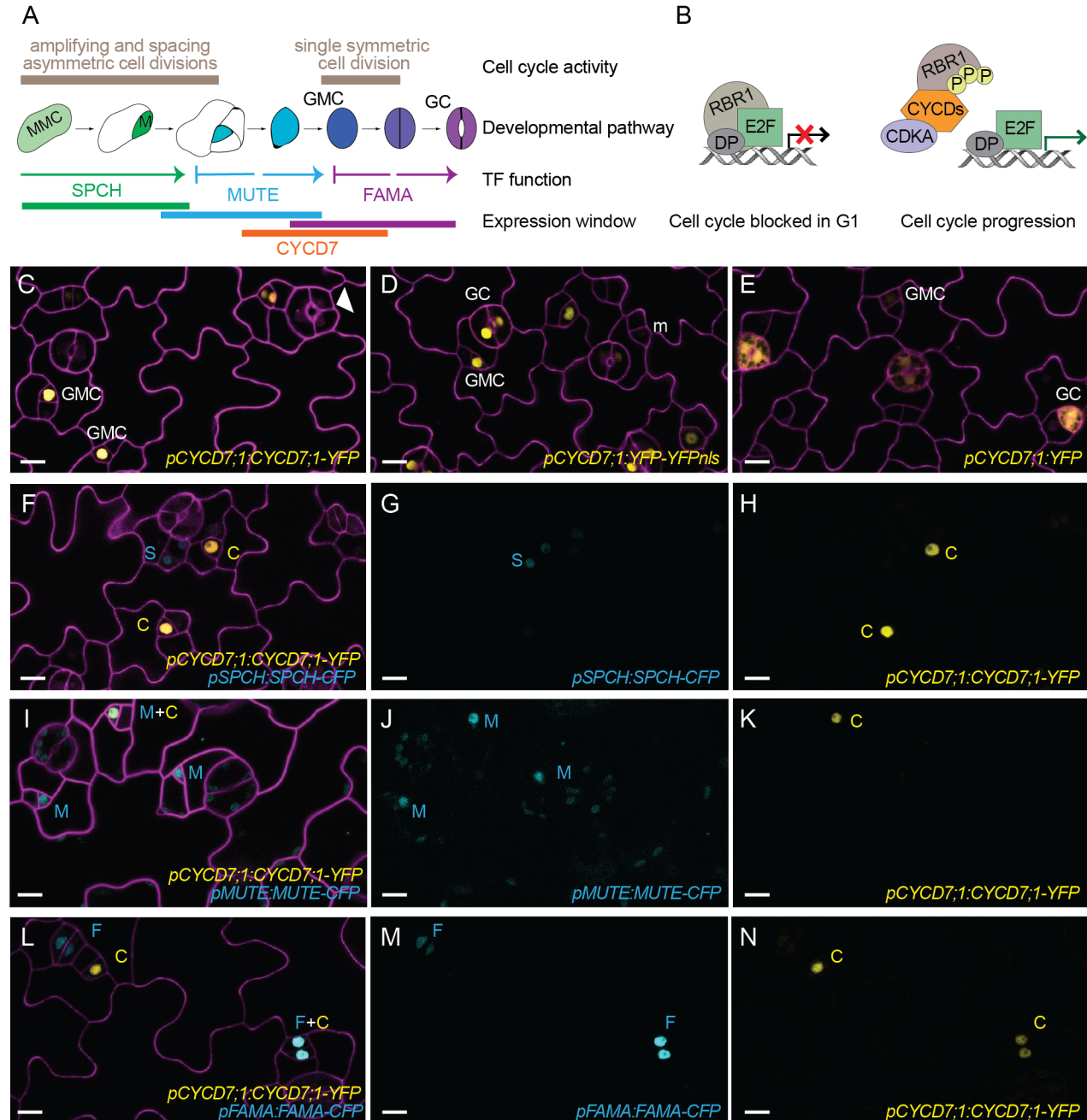


- 464 **MacAlister, C. A., Ohashi-Ito, K. and Bergmann, D. C.** (2007). Transcription factor control of  
465 asymmetric cell divisions that establish the stomatal lineage. *Nature* **445**, 537–540.
- 466 **Matos, J. L. and Bergmann, D. C.** (2014). Convergence of stem cell behaviors and genetic regulation  
467 between animals and plants: insights from the Arabidopsis thaliana stomatal lineage. *F1000Prime*  
468 *Rep* **6**, 53.
- 469 **Matos, J. L., Lau, O. S., Hachez, C., Cruz-Ramírez, A., Scheres, B. and Bergmann, D. C.** (2014).  
470 Irreversible fate commitment in the Arabidopsis stomatal lineage requires a FAMA and  
471 RETINOBLASTOMA-RELATED module. *Elife* **3**, 1792.
- 472 **McElwain, J. C., Yiotis, C. and Lawson, T.** (2016). Using modern plant trait relationships between  
473 observed and theoretical maximum stomatal conductance and vein density to examine patterns of  
474 plant macroevolution. *New Phytologist* **209**, 94–103.
- 475 **Menges, M., Hennig, L., Gruissem, W. and Murray, J. A. H.** (2003). Genome-wide gene expression  
476 in an Arabidopsis cell suspension. *Plant Mol. Biol.* **53**, 423–442.
- 477 **Menges, M., Pavesi, G., Morandini, P., Bögre, L. and Murray, J. A. H.** (2007). Genomic  
478 organization and evolutionary conservation of plant D-type cyclins. *Plant Physiol.* **145**, 1558–1576.
- 479 **Menges, M., Samland, A. K., Planchais, S. and Murray, J. A. H.** (2006). The D-type cyclin  
480 CYCD3;1 is limiting for the G1-to-S-phase transition in Arabidopsis. *The Plant Cell* **18**, 893–906.
- 481 **Nakagami, H., Kawamura, K., Sugisaka, K., Sekine, M. and Shinmyo, A.** (2002). Phosphorylation  
482 of retinoblastoma-related protein by the cyclin D/cyclin-dependent kinase complex is activated at  
483 the G1/S-phase transition in tobacco. *The Plant Cell* **14**, 1847–1857.
- 484 **Nakagawa, T., Nakamura, S., Tanaka, K., Kawamukai, M., Suzuki, T., Nakamura, K., Kimura, T.  
485 and Ishiguro, S.** (2008). Development of R4 Gateway Binary Vectors (R4pGWB) Enabling High-  
486 Throughput Promoter Swapping for Plant Research. *Bioscience, Biotechnology, and Biochemistry*  
487 **72**, 624–629.
- 488 **Nowack, M. K., Harashima, H., Dissmeyer, N., Zhao, X., Bouyer, D., Weimer, A. K., De Winter,  
489 F., Yang, F. and Schnittger, A.** (2012). Genetic framework of cyclin-dependent kinase function in  
490 Arabidopsis. *Dev. Cell* **22**, 1030–1040.
- 491 **Ohashi-Ito, K. and Bergmann, D. C.** (2006). Arabidopsis FAMA controls the final  
492 proliferation/differentiation switch during stomatal development. *Plant Cell* **18**, 2493–2505.
- 493 **Pillitteri, L. J. and Torii, K. U.** (2007). Breaking the silence: three bHLH proteins direct cell-fate  
494 decisions during stomatal development. *BioEssays* **29**, 861–870.
- 495 **Pillitteri, L. J., Sloan, D. B., Bogenschutz, N. L. and Torii, K. U.** (2007). Termination of asymmetric  
496 cell division and differentiation of stomata. *Nature* **445**, 501–505.
- 497 **Riou-Khamlichi, C., Menges, M., Healy, J. M. S. and Murray, J. A. H.** (2000). Sugar Control of the  
498 Plant Cell Cycle: Differential Regulation of Arabidopsis D-Type Cyclin Gene Expression. *Mol.*

- 499 *Cell. Biol.* **20**, 4513–4521.
- 500 **Roeder, A. H. K., Chickarmane, V., Cunha, A., Obara, B., Manjunath, B. S. and Meyerowitz, E.**  
501 **M.** (2010). Variability in the control of cell division underlies sepal epidermal patterning in  
502 *Arabidopsis thaliana*. *PLoS Biol.* **8**, e1000367.
- 503 **Sanz, L., Dewitte, W., Forzani, C., Patell, F., Nieuwland, J., Wen, B., Quelhas, P., De Jager, S.,**  
504 **Titmus, C., Campilho, A., et al.** (2011). The Arabidopsis D-Type Cyclin CYCD2;1 and the  
505 Inhibitor ICK2/KRP2 Modulate Auxin-Induced Lateral Root Formation. *The Plant Cell* **23**, 641–  
506 660.
- 507 **Schellmann, S., Schnittger, A., Kirik, V., Wada, T., Okada, K., Beermann, A., Thumfahrt, J.,**  
508 **Jürgens, G. and Hülskamp, M.** (2002). TRIPTYCHON and CAPRICE mediate lateral inhibition  
509 during trichome and root hair patterning in Arabidopsis. *The EMBO Journal* **21**, 5036–5046.
- 510 **Sozzani, R., Cui, H., Moreno-Risueno, M. A., Busch, W., Van Norman, J. M., Vernoux, T., Brady,**  
511 **S. M., Dewitte, W., Murray, J. A. H. and Benfey, P. N.** (2010). Spatiotemporal regulation of cell-  
512 cycle genes by SHORTROOT links patterning and growth. *Nature* **466**, 128–132.
- 513 **Sterken, R., Kiekens, R., Boruc, J., Zhang, F., Vercauteren, A., Vercauteren, I., De Smet, L.,**  
514 **Dhondt, S., Inzé, D., De Veylder, L., et al.** (2012). Combined linkage and association mapping  
515 reveals CYCD5;1 as a quantitative trait gene for endoreduplication in Arabidopsis. *PNAS* **109**,  
516 4678–4683.
- 517 **Tanaka, Y., Nakamura, S., Kawamukai, M., Koizumi, N. and Nakagawa, T.** (2011). Development  
518 of a series of gateway binary vectors possessing a tunicamycin resistance gene as a marker for the  
519 transformation of Arabidopsis thaliana. *Bioscience, Biotechnology, and Biochemistry* **75**, 804–807.
- 520 **Uemukai, K., Iwakawa, H., Kosugi, S., de Uemukai, S., Kato, K., Kondorosi, E., Murray, J. A., Ito,**  
521 **M., Shinmyo, A. and Sekine, M.** (2005). Transcriptional activation of tobacco E2F is repressed by  
522 co-transfection with the retinoblastoma-related protein: cyclin D expression overcomes this  
523 repressor activity. *Plant Mol. Biol.* **57**, 83–100.
- 524 **Umen, J. G. and Goodenough, U. W.** (2001). Control of cell division by a retinoblastoma protein  
525 homolog in Chlamydomonas. *Genes Dev.* **15**, 1652–1661.
- 526 **Van Leene, J., Hollunder, J., Eeckhout, D., Persiau, G., Van De Slijke, E., Stals, H., Van Isterdael,**  
527 **G., Verkest, A., Neiryneck, S., Buffel, Y., et al.** (2010). Targeted interactomics reveals a complex  
528 core cell cycle machinery in Arabidopsis thaliana. *Molecular Systems Biology* **6**, 397.
- 529 **Vandepoele, K., Raes, J., De Veylder, L., Rouzé, P., Rombauts, S. and Inzé, D.** (2002). Genome-  
530 Wide Analysis of Core Cell Cycle Genes in Arabidopsis. *The Plant Cell* **14**, 903–916.
- 531 **Vanneste, S., Coppens, F., Lee, E., Donner, T. J., Xie, Z., Van Isterdael, G., Dhondt, S., De Winter,**  
532 **F., De Rybel, B., Vuylsteke, M., et al.** (2011). Developmental regulation of CYCA2s contributes to  
533 tissue-specific proliferation in Arabidopsis. *The EMBO Journal* **30**, 3430–3441.
- 534 **Wang, G., Kong, H., Sun, Y., Zhang, X., Zhang, W., Altman, N., DePamphilis, C. W. and Ma, H.**

- 535 (2004). Genome-wide analysis of the cyclin family in Arabidopsis and comparative phylogenetic  
536 analysis of plant cyclin-like proteins. *Plant Physiol.* **135**, 1084–1099.
- 537 **Weimer, A. K., Biedermann, S., Harashima, H., Roodbarkelari, F., Takahashi, N., Foreman, J.,**  
538 **Guan, Y., Pochon, G., Heese, M., Van Damme, D., et al.** (2016). The plant-specific CDKB1-  
539 CYCB1 complex mediates homologous recombination repair in Arabidopsis. *The EMBO Journal*  
540 **35**, 2068–2086.
- 541 **Weimer, A. K., Nowack, M. K., Bouyer, D., Zhao, X., Harashima, H., Naseer, S., De Winter, F.,**  
542 **Dissmeyer, N., Geldner, N. and Schnittger, A.** (2012). Retinoblastoma related1 regulates  
543 asymmetric cell divisions in Arabidopsis. *Plant Cell* **24**, 4083–4095.
- 544 **Xie, Z., Lee, E., Lucas, J. R., Morohashi, K., Li, D., Murray, J. A. H., Sack, F. D. and Grotewold,**  
545 **E.** (2010). Regulation of cell proliferation in the stomatal lineage by the Arabidopsis MYB FOUR  
546 LIPS via direct targeting of core cell cycle genes. *Plant Cell* **22**, 2306–2321.
- 547 **Zhao, X., Harashima, H., Dissmeyer, N., Pusch, S., Weimer, A. K., Bramsiepe, J., Bouyer, D.,**  
548 **Rademacher, S., Nowack, M. K., Novak, B., et al.** (2012). A general G1/S-phase cell-cycle  
549 control module in the flowering plant Arabidopsis thaliana. *PLoS Genet.* **8**, e1002847.

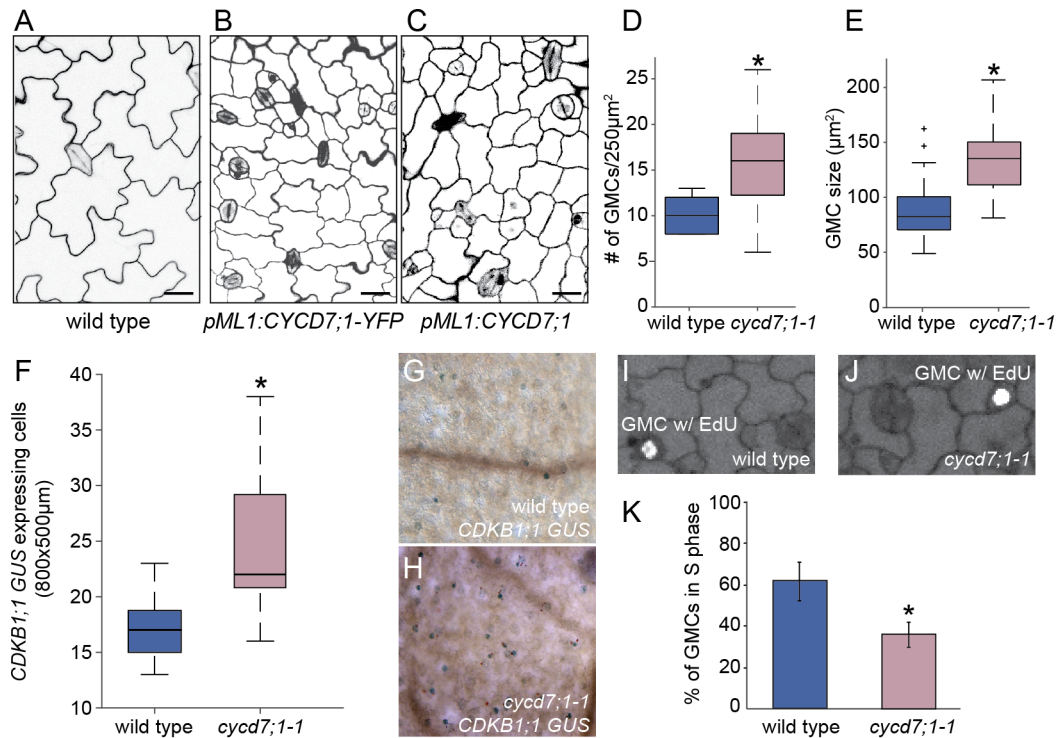
550 **Figures and Figure legends**



551  
 552 **Figure 1: CYCD7;1 is expressed in GMCs prior to the last symmetric division of the stomatal**  
 553 **lineage**

554 (A) Scheme of stomatal development in *Arabidopsis thaliana*. Cell cycle activity depicted in beige, with  
 555 cell fate transitions, function and expression window of master bHLH transcription factors SPCH  
 556 (green), MUTE (blue), and FAMA (purple) and CYCD7;1 (orange). Meristemoid mother cells (light

557 green, MMC) divide asymmetrically to enter the lineage. Meristemoids (green) can undergo amplifying  
558 and spacing asymmetric cell divisions until activity is terminated. Guard mother cells (GMC, blue)  
559 reenter the cell cycle only once to generate the pair of symmetric guard cells (GC, purple). **(B)** Cartoon  
560 of plant RBR1/CYCD complexes driving the G1 to S transition and commitment to divide. RBR1 binds  
561 to E2F-DP transcription factors and blocks their ability to induce transcription of S phase genes. CYCDs  
562 interact with RBR1 through their LxCxE motif and facilitate phosphorylation of RBR1 by the  
563 CDKA;1/CYCD complex. Upon phosphorylation RBR1 releases E2F transcription factors, which leads  
564 to expression of S phase genes for DNA replication. **(C-E)** Expression of the translational reporter  
565 *pCYCD7;1:CYCD7;1-YFP*, the transcriptional reporters *pCYCD7;1:YFP-YFPnls* and *pCYCD7;1:YFP*  
566 (all yellow) in abaxial cotyledons. White arrowheads point at ectopic cell divisions. **(F-N)** Co-  
567 expression of *pCYCD7;1:CYCD7;1-YFP* (yellow, C) and *pSPCH:SPCH-CFP* (cyan, S),  
568 *pMUTE:MUTE-CFP* (cyan, M) and *pFAMA:FAMA-CFP* (cyan, F).  
569  
570 Confocal images were taken at 5 dag (days after germination). Cell outlines (magenta) are visualized  
571 with propidium iodide. All images are at the same magnification and scale bar is 10 $\mu$ M.

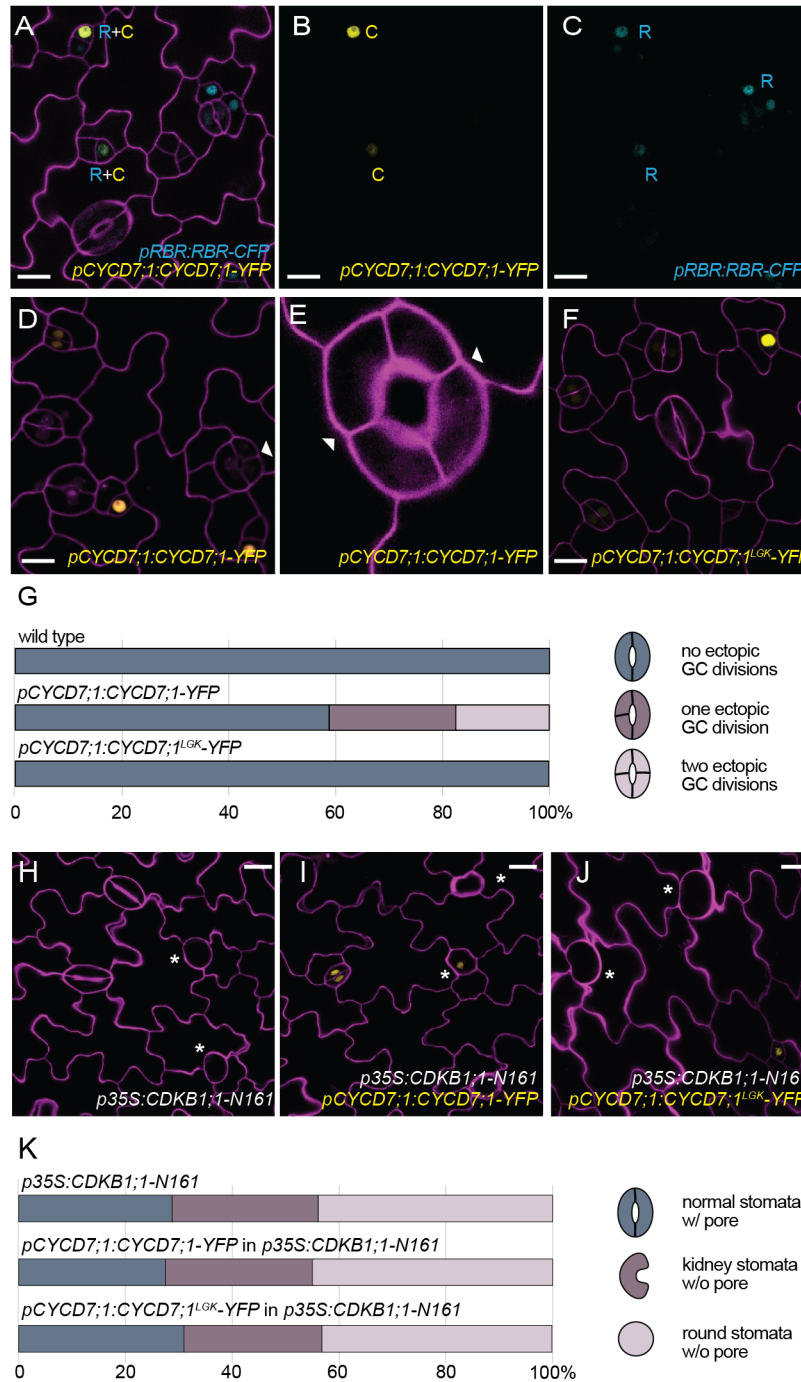


572

573 **Figure 2: CYCD7;1 promotes cell divisions**

574 (A-C) Confocal images of adaxial cotyledon epidermes of wild type, and plant expressing  
575 *pML1:CYCD7;1-YFP* and *pML1:CYCD7;1* at 6 dag. Cell outlines were visualized with propidium  
576 iodide (magenta). Scale bar 20µM. (D) Quantification of the number of GMCs in wild type and *cycd7;1-1*  
577 *1* cotyledons at 4 dag. Asterisk indicates significant difference (p-value = 0.0032; Mann-Whitney U  
578 test). (E) Quantification of GMC area in wild type (N=55) and *cycd7;1-1* (N=51) cotyledons at 4 dag.  
579 Asterisk indicates significant difference (p-value = 6.76E-13; Mann-Whitney U test). (F) Quantification  
580 of cells expressing the *CDKB1;1-GUS* marker in wild type and *cycd7;1-1* cotyledons at 5 dag. Asterisk  
581 indicates significant difference (p-value = 0.0023; Mann-Whitney U test). (G) Image of wild type  
582 cotyledon expressing *CDKB1;1-GUS* marker at 5 dag. (H) Image of *cycd7;1-1* cotyledon expressing  
583 *CDKB1;1-GUS* marker at 5 dag. (I) Image of wild type GMC with EdU (5-ethynyl-2'-deoxyuridine)  
584 labeling at 4 dag cotyledon. (J) Image of *cycd7;1-1* GMC with EdU labeling, 4-day old cotyledon. (K)  
585 Quantification of EdU labeling in wild type and *cycd7;1-1* mutants. Graph shows the % of GMCs in S  
586 phase during a 90-minute incubation with EdU. Error bars indicate the 95% confidence interval.  
587 Asterisk indicates significant difference (p-value = 7x10E-6; Fisher's Exact Test).

588 Center lines in box plots show the medians; box limits indicate the 25th and 75th percentiles; whiskers  
589 extend 1.5 times the interquartile range from the 25th and 75th percentiles.



590

591 **Figure 3: CYCD7;1 requires RBR1 binding and CDKB1;1 activity for ectopic cell divisions**

592 (A-C) Co-expression of *pCYCD7;1:CYCD7;1-YFP* (yellow, C) and *pRBR1:RBR1-CFP* (cyan, R) in

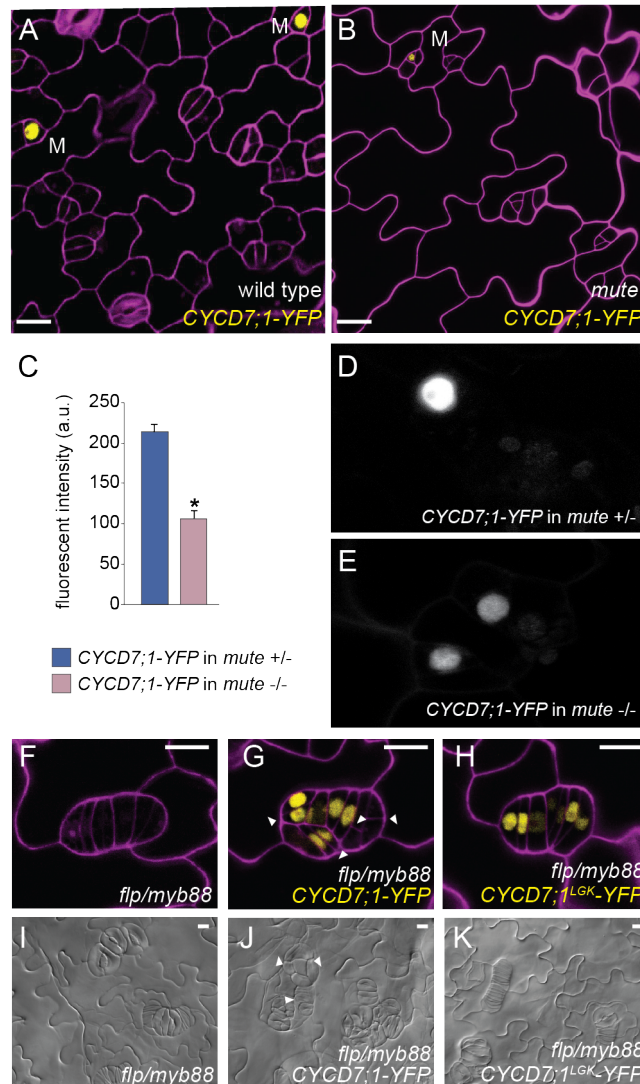
593 GMCs at 5 dag. (D-E) Expression of *pCYCD7;1:CYCD7;1-YFP* drives ectopic cell divisions (white

594 arrowheads). (F) Expression of *pCYCD7;1:CYCD7;1<sup>LGK</sup>-YFP* (yellow) does not drive ectopic cell

595 divisions. (G) Quantification of ectopic cell divisions in GCs at 5 dag in cotyledons in wild type

596 (N=173), *pCYCD7;1:CYCD7;1-YFP* (N=306) and *pCYCD7;1:CYCD7;1<sup>LGK</sup>-YFP* (N=288). **(H)**  
597 Phenotype of dominant negative *p35S:CDKB1;1-N161* at 6 dag. White asterisks label arrested GMCs.  
598 **(I-J)** Failure of *pCYCD7;1:CYCD7;1-YFP* (I) and *pCYCD7;1:CYCD7;1<sup>LGK</sup>-YFP* (J) to suppress  
599 *CDKB1;1-N161* phenotype at 6 dag. White asterisks label arrested GMCs. **(K)** Quantification of stomata  
600 phenotypes in cotyledons in *p35S:CDKB1;1-N161* (N=238), *pCYCD7;1:CYCD7;1-YFP* in  
601 *p35S:CDKB1;1-N161* (N=296) and *pCYCD7;1:CYCD7;1<sup>LGK</sup>-YFP* in *p35S:CDKB1;1-N161* (N=217) at  
602 6 dag.  
603 Confocal images show cell outlines (magenta) stained with propidium iodide. Scale bar 10  $\mu$ m (A-D, F)  
604 and 20  $\mu$ m (H-J).





605

606 **Figure 4: CYCD7;1-YFP is expressed at low levels in *mute* mutants and persists and drives ectopic**  
607 **divisions in *flp/myb88* mutants**

608 (A, B) Wild type and *mute* mutants expressing *pCYCD7;1::CYCD7;1-YFP* in 6 day old cotyledons. Scale  
609 bar 10 μm; M, meristemoid. (C-E) Quantification of fluorescence intensity of CYCD7;1-YFP in

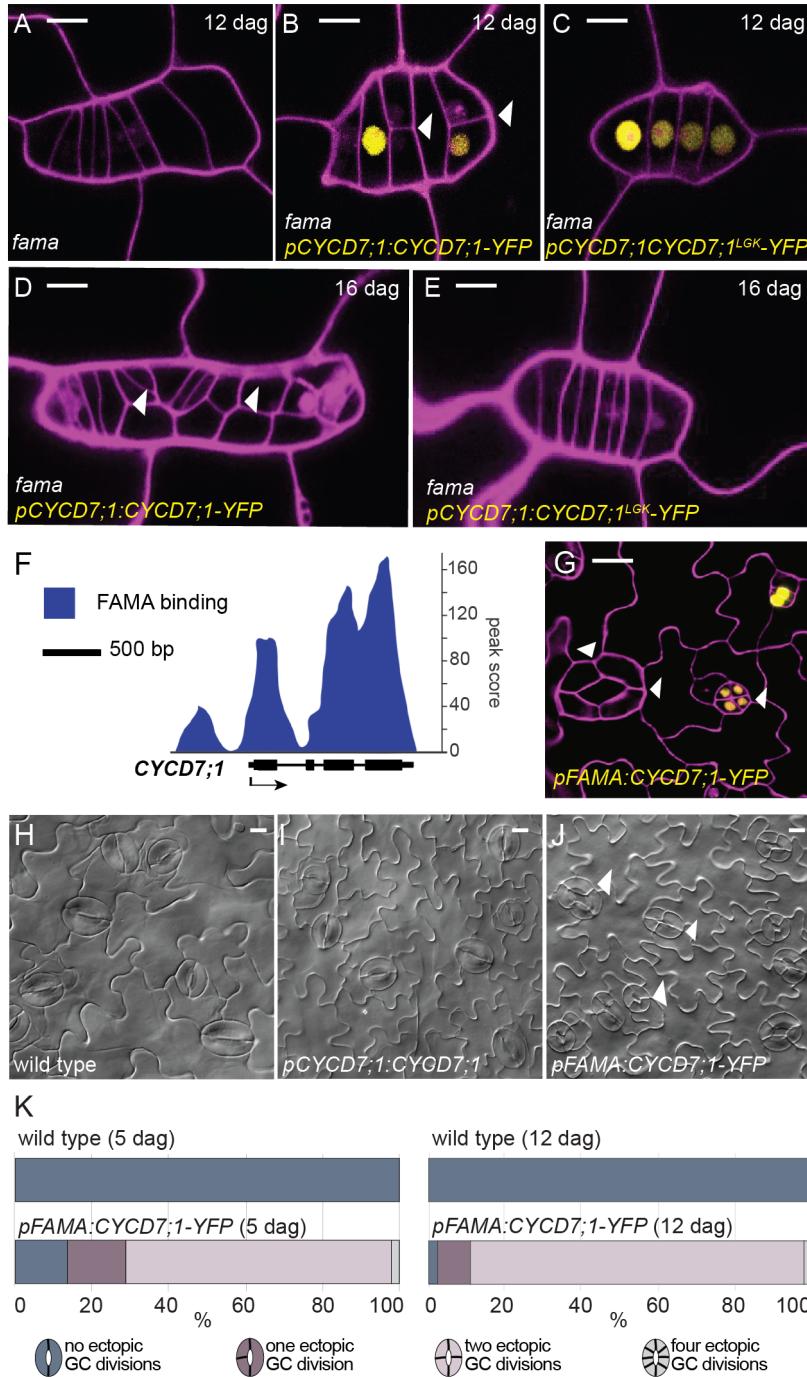
610 homozygous *mute* mutants (N=27) and their heterozygous or wild-type sister plants (N=21) (a.u.,  
611 arbitrary units). Images of cotyledons were taken at 4 dag. Error bars show standard error. Asterisk

612 shows statistical significance (p-value <0.0001; Student-t test). (F) Phenotype of the double mutant  
613 *flp/myb88* at 6 dag. (G) Expression of *pCYCD7;1::CYCD7;1-YFP* in *flp/myb88* drives ectopic divisions

614 in tumors at 6 dag. (H) Expression of *pCYCD7;1::CYCD7;1<sup>LGK</sup>-YFP* in *flp/myb88* is less able to drive  
615 ectopic divisions at 6 dag. (I) DIC images of the phenotype of the double mutant *flp/myb88* at 12 dag.

616 (J) Expression of *pCYCD7;1::CYCD7;1-YFP* in *flp/myb88* drives ectopic divisions in tumors at 12 dag.

617 **(K)** Expression of *pCYCD7;1:CYCD7;1<sup>LGK</sup>-YFP* in *flp/myb88* is less able to drive ectopic divisions at  
618 12 dag. White arrowheads label ectopic divisions. Confocal images show cell outlines (magenta) stained  
619 with propidium iodide. Scale bar 10 $\mu$ M.



620

621 **Figure 5: CYCD7;1 expression is regulated by FAMA which serves to constrain CYCD7;1 activity**

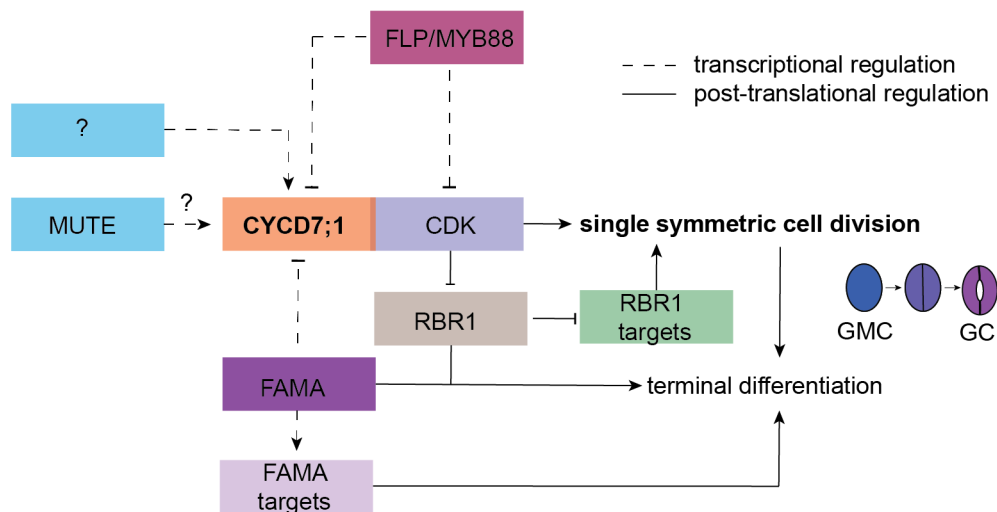
622 (A-E) Confocal images of *fama*, *pCYCD7;1:CYCD7;1-YFP* in *fama* mutant background and

623 *pCYCD7;1:CYCD7;1<sup>LGK</sup>-YFP* in *fama* mutant background at 12 or 16 dag, respectively. (F) ChIP-Seq

624 profile of FAMA binding to the promoter and gene body of *CYCD7;1*. Black arrow indicates gene

625 orientation and transcriptional start sites. (G) Confocal image of *pFAMA:CYCD7;1-YFP* at 5 dag. White

626 arrowheads show ectopic division and prolonged *CYCD7;1*-YFP presence. **(H-J)** DIC images of abaxial  
627 cotyledon epidermis of wild type, *pCYCD7;1:CYCD7;1* and *pFAMA:CYCD7;1-YFP* at 12 dag. Scale  
628 bar, 10 $\mu$ M. Arrowheads point at ectopic cell divisions. **(K)** Quantification of ectopic cell divisions in  
629 wild type (N=142) and *pFAMA:CYCD7;1-YFP* (N=237) at 5 dag and in wild type (N=125) and  
630 *pFAMA:CYCD7;1-YFP* (N=153) at 12 dag. Confocal images show cell outlines (magenta) stained with  
631 propidium iodide. Scale bar 10 $\mu$ m.

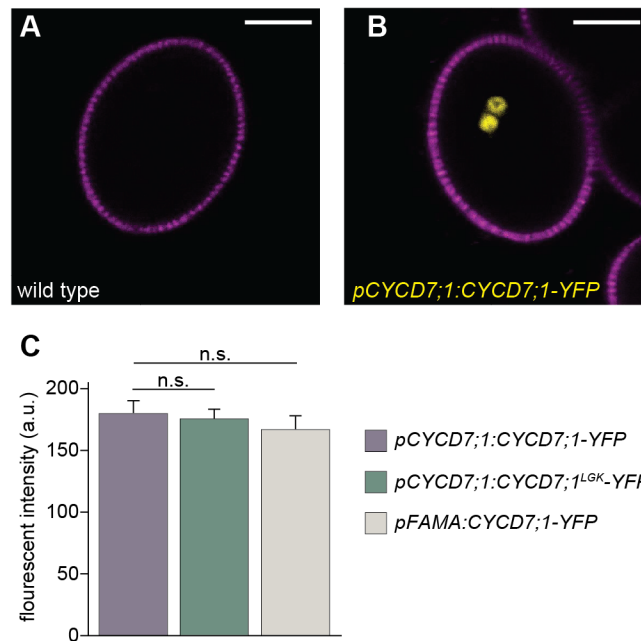


632

633 **Figure 6: Model of the developmental integration of CYCD7;1 to ensure lineage specific cell cycle**  
 634 **regulation**

635 Cell cycle regulators are integrated with stomatal specific transcriptions factors to ensure the last  
 636 formative division of the lineage that creates one pair of symmetric guard cells. Initiation of CYCD7;1's  
 637 expression in GMCs requires factors in addition to MUTE (question mark). CYCD7;1 together with its  
 638 CDK partner executes the formative division of the GMC. Due to the observation that this last division  
 639 is not completely abolished in *cycd7;1* mutants, other D-type cyclins likely back up G1-S phase  
 640 transition. CDK/CYCD complexes phosphorylate RBR1 in order to release its negative function on S  
 641 phase promoting factors. To ensure termination of the lineage, the transcription factor FAMA, itself  
 642 slightly later expressed than CYCD7;1, binds to the CYCD7;1 promoter to temporally control  
 643 expression of the lineage-specific CYCD7;1 to GMCs and to restrict the cell cycle right after the last  
 644 division. Transcriptional regulation is marked by dashed lines. This regulatory network ensures high cell  
 645 cycle activity for the last formative division in the stomatal lineage and terminates cell division activity  
 646 to “one and only one” division.

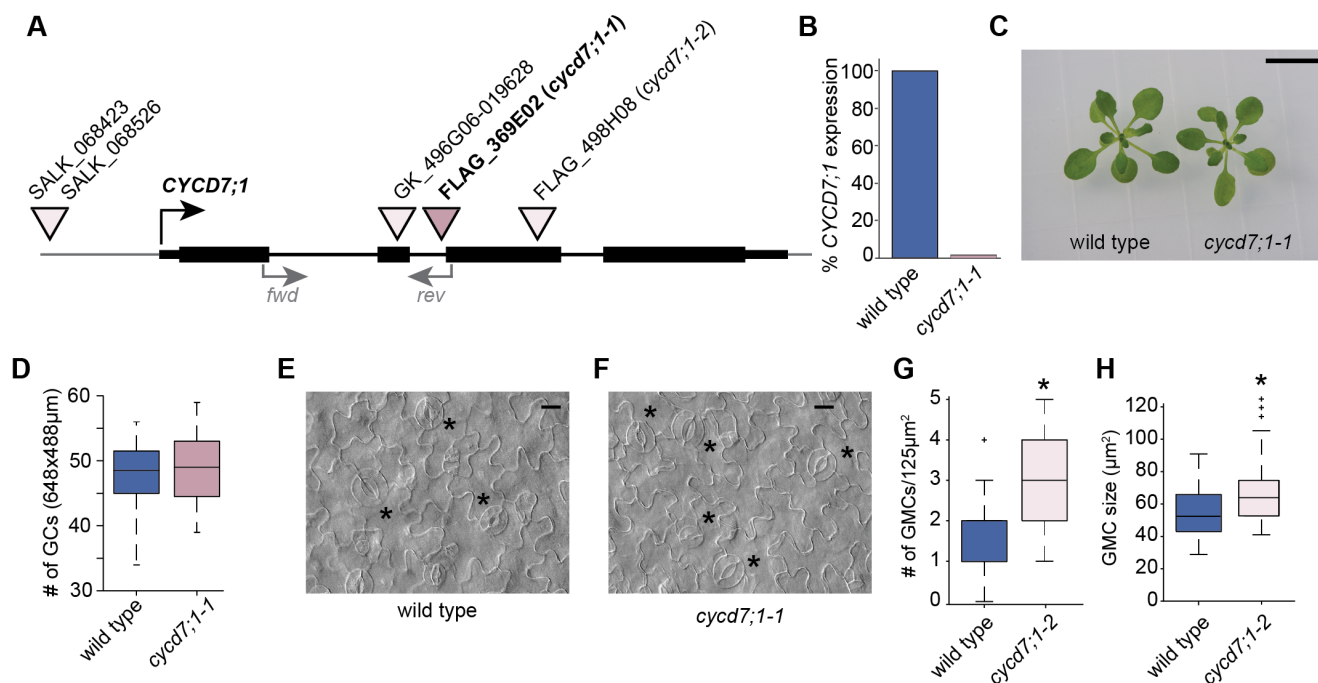
647 **Supplementary Figures**



648

649 **Figure S1: CYCD7;1 expression patterns**

650 **(A, B)** CYCD7;1 (yellow) is expressed in sperm cells during pollen anthesis. **(C)** Intensity  
651 measurements of fluorescent nuclei were 179 a.u. +/-10 SE for *proCYCD7;1:CYCD7;1-YFP* vs 176 a.u.  
652 +/-8 SE for *proCYCD7;1:CYCD7;1<sup>Lgk</sup>-YFP* (N=15 nuclei/line;  $p > 0.05$ ; Student's t-test) and  
653 *proCYCD7;1:CYCD7;1-YFP* 166 a.u. +/-11 SE for *proFAMA:CYCD7;1-YFP* (N=15 nuclei/line;  $p >$   
654 0.05; Student's t-test). Error bars show standard error. a.u., arbitrary units; n.s. non-significant; SE,  
655 standard error.



656

657 **Figure S2: T-DNA insertion lines and phenotype of *cycd7;1* mutants**

658 (A) Schematic drawing of *CYCD7;1* gene structure with available T-DNA insertion lines and their  
659 insertion sites. Black boxes indicate exons. Gray arrowheads marked with *fwd* and *rev* show primer  
660 binding sites for qPCR. (B) qPCR of *CYCD7;1* expression in wild type and the *cycd7;1-1* mutant.  
661 Primer binding sites are shown in (A). (C) Wild type and *cycd7;1-1* mutant seedlings at 14 dag. (D)  
662 Quantification of GCs in wild type and *cycd7;1-1* mutants at 5 dag on the abaxial side of cotyledons (N  
663 =12 cotyledons for each genotype). Difference between the wild type and *cycd7;1-1* is not significant (p-  
664 value = 0.8169; Mann-Whitney U test). (E) Wild type cotyledon with mature GCs, labeled with black  
665 asterisks at 7 dag. (F) Cotyledon of *cycd7;1-1* mutant with mature GCs, labeled with black asterisks,  
666 images were taken at 7 dag. (G) Quantification of the number of GMCs in wild type and *cycd7;1-2*  
667 cotyledons at 4 dag. Asterisk indicates significant difference (p-value = 0.0031; Mann-Whitney U test).  
668 (H) Quantification of GMC area in wild type (N=29) and *cycd7;1-2* (N=46) cotyledons, 4 dag. Asterisk  
669 indicates significant difference (p-value = 0.0053; Mann-Whitney U test).  
670 Center lines show the medians; box limits indicate the 25th and 75th percentiles; whiskers extend 2.5  
671 times the interquartile range from the 97.5th percentile. Scale bar 1 cm in (C) and 20 µM in (E and F).